QUASIFUCHSIAN STATE SURFACES

DAVID FUTER, EFSTRATIA KALFAGIANNI, AND JESSICA S. PURCELL

Abstract. This paper continues our study, initiated in [13], of essential state surfaces in link complements that satisfy a mild diagrammatic hypothesis (homogeneously adequate). For hyperbolic links, we show that the geometric type of these surfaces in the Thurston trichotomy is completely determined by a simple graph–theoretic criterion in terms of a certain spine of the surfaces. For links with A– or B–adequate diagrams, the geometric type of the surface is also completely determined by a coefficient of the colored Jones polynomial of the link.

1. Introduction

A major goal in modern knot theory is to relate the geometry of a knot complement to basic topological invariants that are easy to read off a diagram of the knot. In a recent monograph [13], we find connections between geometric invariants of a knot or link complement, combinatorial properties of its diagram, and stable coefficients of its colored Jones polynomials. The bridge among these different invariants consists of *state surfaces* associated to Kauffman states of a link diagram [17]. These surfaces lie in the link complement and are naturally constructed from a diagram, while certain graphs that form a spine for these surfaces aid in the computation of Jones polynomials [7].

In this paper, we continue the study of these state surfaces, with the goal of obtaining additional geometric information on a link complement, and relating it back to diagrammatical and quantum invariants of the link. In particular, we establish combinatorial criteria that characterize the geometric types of state surfaces in the Thurston trichotomy. This trichotomy, proved by Thurston [26] and Bonahon [2], asserts that every essential surface in a hyperbolic 3-manifold fits into exactly one of three types: semi-fiber, quasifuchsian, or accidental. (See Definition 1.2 below for details.) We show that under a mild diagrammatic hypothesis, certain state surfaces will never be accidental, and a simple graph–theoretic property determines whether the state surface is a semi-fiber or quasifuchsian. For the class of A– or B–adequate diagrams, which arise in the study of knot polynomial invariants [19, 25], the geometric type of the surface is determined by the colored Jones polynomials of the knot. See Theorem 1.4 below.

The problem of determining the geometric types of essential surfaces in knot and link complements has been studied fairly well in the literature. For example, Menasco and Reid proved that no alternating link complement contains an embedded quasifuchsian closed

D.F. is supported in part by NSF grant DMS–1007221.
E.K. is supported in part by NSF grant DMS–1105843.
J.P. is supported in part by NSF grant DMS–1007437 and a Sloan Research Fellowship.
October 25, 2013.

surface [21], which led to the result that there are no embedded totally geodesic surfaces in alternating link complements. More recently, Masters and Zhang found closed, immersed quasifuchsian surfaces in any hyperbolic link complement [20]. As for accidental surfaces, Finkelstein and Moriah established conditions for the existence of closed accidental surfaces in a wide range of link complements [10, 11]. This work was generalized by Wu [30].

Turning to surfaces with boundary, it is known that all three geometric types occur in hyperbolic link complements. For example, Tsutsumi constructed hyperbolic knots with accidental Seifert surfaces of arbitrarily high genus [27]. On the other hand, Fenley proved that minimal genus Seifert surfaces cannot be accidental [9]. An alternate proof of this was given by Cooper and Long [5]. Wise showed that checkerboard surfaces in alternating link complements are not virtual fibers [29], and Adams showed that they are always quasifuchsian [1]. Here we give an alternate proof of this fact, and provide broad families of non-accidental surfaces constructed from non-alternating diagrams.

The results of this paper have some direct consequences in hyperbolic geometry. First, they dovetail with recent work of Thistlethwaite and Tsvietkova, who gave an algorithm to construct the hyperbolic structure on a link complement directly from a diagram [24, 28]. Their algorithm works whenever a link diagram admits a non-accidental state surface, which is exactly what our results ensure for a very large class of diagrams. Second, the quasifuchsian surfaces that we construct fit into the machinery developed by Adams [1]. He showed that if a cusped hyperbolic manifold contains a properly embedded quasifuchsian surface with boundary, then there are restrictions on the cusp geometry of that manifold.

1.1. **Definitions and main results.** To describe our results precisely, we need some definitions. As we will be working with both orientable and non-orientable surfaces, we need to clarify the notion of an essential surface.

Definition 1.1. Let M be an orientable 3–manifold and $S \subset M$ a properly embedded surface. We say that S is *essential* in M if the boundary of a regular neighborhood of S, denoted $\widetilde{S}$, is incompressible and boundary–incompressible.

Note that if S is orientable, then $\widetilde{S}$ consists of two copies of S, and the definition is equivalent to the standard notion of "incompressible and boundary–incompressible" for orientable surfaces.

Definition 1.2. Let M be a compact 3–manifold with boundary consisting of tori, and let S be a properly embedded essential surface in M. An *accidental parabolic* on S is a free homotopy class of a closed curve that is not boundary–parallel on S but can be homotoped to the boundary of M. If M is hyperbolic, then the embedding of S into M induces a faithful representation $\rho\colon \pi_1(S) \hookrightarrow \pi_1(M) \subset PSL(2,\mathbb{C})$. In this case, an *accidental parabolic* is a non-peripheral element of $\pi_1(S)$ that is is mapped by ρ to a parabolic in $\pi_1(M)$. A surface S with accidental parabolics is called *accidental*.

If M is hyperbolic, the surface S is called *quasifuchsian* if the embedding $S \hookrightarrow M$ lifts to a topological plane in $\mathbb{H}^3$ whose limit set $\Lambda \subset \partial\mathbb{H}^3$ is a topological circle. Note that we permit S to be non-orientable: in this case, the two disks bounded by the Jordan curve Λ will be be interchanged by isometries corresponding to $\pi_1(S)$.

Finally, we say the surface S is a *semi-fiber* if it is a fiber in M or covered by a fiber in a two-fold cover of M. If S is a semi-fiber but not a fiber, we call it a *strict* semi-fiber.

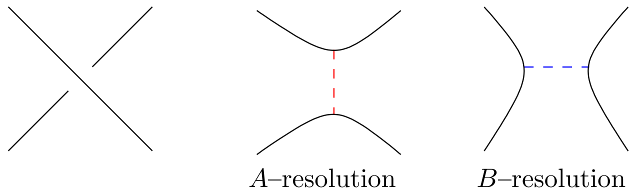

FIGURE 1. A– and B–resolutions of a crossing.

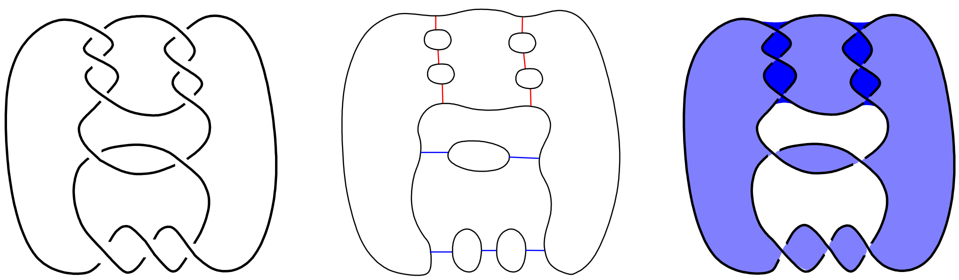

FIGURE 2. Left: A link diagram. Center: the graph H_σ corresponding to an adequate, homogeneous state σ. Right: state surface S_σ.

By the work of Thurston [26] and Bonahon [2] (see also Canary, Epstein and Green [3]), every properly embedded, essential surface S in a hyperbolic 3–manifold M falls into exactly one of the three types in Definition 1.2: S is either a semi-fiber, or accidental, or quasifuchsian.

We will apply the above definitions to surfaces constructed from *Kauffman states* of link diagrams. For any crossing of a link diagram $D(K)$, there are two associated diagrams, obtained by removing the crossing and reconnecting the diagram in one of two ways, called the *A–resolution* and *B–resolution* of the crossing, shown in Figure 1.

A choice of A– or B–resolution for each crossing of D is called a *Kauffman state* [17]. The result of applying a Kauffman state σ to a link diagram D is a collection of circles s_σ disjointly embedded in the projection plane $S^2 \subset S^3$. These circles bound embedded disks whose interiors can be made disjoint by pushing them below the projection plane. Now, at each crossing of D, we connect the pair of neighboring disks by a half–twisted band to construct a *state surface* $S_\sigma \subset S^3$ whose boundary is K.

State surfaces generalize the classical checkerboard knot surfaces, and they have recently appeared in the work of several authors, including Przytycki [23] and Ozawa [22]. They are the primary object of interest in this paper, for certain states. In order to describe these states, we need a few more definitions.

From the collection of state circles s_σ we obtain a trivalent graph H_σ by attaching edges, one for each crossing of the original diagram $D(K)$, as shown by the dashed lines of Figure 1. As in [13], the edges of H_σ that come from crossings of the diagram are referred to as *segments*, and the other edges are portions of state circles. See Figure 2.

In the literature, a graph that is more common than the graph H_σ is the *state graph* G_σ, which is formed from H_σ by collapsing components of s_σ to vertices. Remove redundant edges between vertices to obtain the *reduced state graph* G'_σ.

Definition 1.3. Following Lickorish and Thistlethwaite [19, 25], a state σ of a diagram D is said to be *adequate* if every segment of H_σ has its endpoints on distinct state circles of s_σ. In this case, the diagram D is called σ–adequate. When σ is the all–A state (all–B state), we call the diagram A–adequate (B–adequate).

In any state σ, the circles of $s_\sigma(D)$ divide the projection plane into components. Every crossing of D is associated to a segment of H_σ, which belongs to one of these components. Label each segment A or B, in accordance with the choice of resolution at this crossing. We say that the state σ is *homogeneous* if all edges in a complementary region of s_σ have the same A or B label. In this case, we say that D is *σ–homogeneous*. An example is shown in Figure 2. If a link K admits a diagram that is both σ–homogeneous and σ–adequate, for the same state σ, we call K *homogeneously adequate*.

Ozawa showed that the state surface S_σ of an adequate, homogeneous state σ is essential in the link complement [22]. A different proof of this fact follows from machinery developed by the authors [13]. The state surfaces S_A and S_B corresponding to the all–A and all–B states, respectively, also play a significant role in quantum topology. In [13], we show that coefficients of the colored Jones polynomials detect topological information about these surfaces. For instance, if K is an A–adequate link then S_A is a fiber in the link complement precisely when a particular coefficient vanishes (and similarly for S_B).

In this paper, we show that for hyperbolic link complements, the colored Jones polynomial completely determines the geometric type of S_A in the Thurston trichotomy of Definition 1.2. To state our result, let

$$J^n_K(t) = \alpha_n t^{m_n} + \beta_n t^{m_n - 1} + \ldots + \beta'_n t^{r_n+1} + \alpha'_n t^{r_n},$$

denote the n-th *colored Jones polynomial* of a link K, where m_n and r_n denote the highest and the lowest degree. Recall that $J^2_K(t)$ is the usual Jones polynomial. Suppose that K is a link admitting an A–adequate diagram D. Consider the all–A state graph $\mathbb{G}_A$ and the reduced graph $\mathbb{G}'_A$. By [8, Theorem 3.1], for all $n > 1$, we have $|\alpha'_n| = 1$ and $|\beta'_n| = 1 - \chi(\mathbb{G}'_A)$. Thus we may define the *stable coefficient*

$$\beta'_K \;:=\; \left|\beta'_n\right| \;=\; 1 - \chi(\mathbb{G}'_A). \tag{1}$$

Similarly, if D is B–adequate, then $|\alpha_n| = 1$ and $|\beta_n| = 1 - \chi(\mathbb{G}'_B)$, hence there is a stable coefficient $\beta_K := |\beta_n| \;=\; 1 - \chi(\mathbb{G}'_B) = 1 - \chi(\mathbb{G}'_B)$.

Finally, recall that a link diagram D is called *prime* if any simple closed curve that meets the diagram transversely in two points bounds a region of the projection plane without any crossings. A prime knot or link admits a prime diagram.

One of our results is the following theorem.

Theorem 1.4. *Let $D(K)$ be a prime, A–adequate diagram of a hyperbolic link K. Then the stable coefficient β'_K determines the geometric type of the all–A surface S_A, as follows:*

- *If $\beta'_K = 0$, then S_A is a fiber in $S^3 \smallsetminus K$.*
- *If $\beta'_K \neq 0$, then S_A is quasifuchsian.*

Similarly, if $D(K)$ is a prime B–adequate diagram of a hyperbolic link K, then the stable coefficient β_K determines the geometric type of S_B. This surface will be a fiber if $\beta_K = 0$, and quasifuchsian otherwise.

Remark 1.5. The class of A– or B–adequate links includes all alternating links, positive and negative closed braids, closed 3–braids, Montesinos links, Conway sums of alternating tangles and planar cables of all the above. It also includes all but a handful of prime knots up to 12 crossings. See [13, Section 1.3] for more discussion and references. The class of homogeneously adequate links includes all of the above and also contains the homogeneous links studied by Cromwell [6].

We note that the class of homogeneously adequate links is strictly larger than that of A– and B–adequate links: For example, consider the knot $K = 12n0873$ of Knotinfo [4]. Its Jones polynomial $J_K(t) = 3t^{-4} - 7t^{-3} + 11t^{-2} - 14t^{-1} + 15 - 14t + 11t^2 - 7t^3 + 3t^4$ is not monic, hence K is neither A– nor B–adequate. On the other hand, according to [4], K is written as the closure of the homogeneous braid $b = \sigma_1\sigma_2\sigma_3^{-1}\sigma_4^{-1}\sigma_2\sigma_3^{-1}\sigma_1\sigma_2\sigma_3^{-1}\sigma_2\sigma_4^{-1}\sigma_3^{-1}$, where σ_i denotes the i-th standard generator of the 5–string braid group. It is not hard to see that the Seifert state of the closed braid diagram is homogeneous and adequate.

At this writing, it is not known whether *every* hyperbolic link admits a homogeneously adequate diagram. See [22] and [13, Chapter 10] for related discussion and questions.

The main new result of this paper is the following theorem.

Theorem 1.6. *Let $D(K)$ be a prime link diagram with an adequate, homogeneous state σ. Then the state surface S_σ is essential, and admits no accidental parabolics. Furthermore, S_σ is a semi-fiber whenever it is a fiber, which occurs if and only if G'_σ is a tree.*

Theorem 1.4 follows immediately from Theorem 1.6: simply restrict to A–adequate diagrams, and note that equation (1) above implies $\beta'_K = 0$ precisely when $\mathbb{G}'_A$ is a tree.

The result that checkerboard surfaces in hyperbolic alternating link complements are quasifuchsian (compare Adams [1]) also follows immediately from Theorem 1.6. This is because checkerboard surfaces correspond to the all–A and all–B states of alternating link complements, which are always homogeneous and adequate, and the corresponding graphs G'_A and G'_B will be trees only when the reduced alternating diagram of the link is a $(2, q)$ torus link, which is not hyperbolic.

The main novel content of Theorem 1.6 is that S_σ is never accidental. Indeed, in [13, Theorem 5.21], we showed that S_σ is a fiber precisely when the reduced state graph G'_σ is a tree and that it is never a strict semi-fiber. Thus, by Thurston and Bonahon [2], for a hyperbolic link K the surface S_σ is quasifuchsian precisely when G'_σ is not a tree.

1.2. **Organization.** In Section 2, we discuss accidental parabolic elements in the fundamental group of a state surface. We observe that the existence of such elements gives rise to an essential embedded annulus in the complement of the state surface, and then exclude such annuli in in the case where K is a knot (see Theorem 2.6). This, in particular, implies the main results for knots.

Proving Theorem 1.6 in the more general case of links is harder, and involves knowing more details about the complement of the state surface. In Section 3, we describe the structure of an ideal decomposition of the state surface complement, which was first constructed in [13]. In Section 4, we study normal annuli in this polyhedral decomposition, and prove that such an annulus can never realize an accidental parabolic. We expect that some of the combinatorial results established in Section 4 will also prove useful for studying more general essential surfaces in the complements of homogeneously adequate links.

2. Embedded annuli and knots

In this section, we prove that if an essential state surface S_σ has an accidental parabolic, that is, if a non-peripheral curve in S_σ is homotopic to the boundary, then such a homotopy can be realized by an embedded annulus. This will quickly lead to a proof of Theorem 1.6 in the special case where K is a knot.

Definition 2.1. Let M be a compact orientable 3–manifold with ∂M consisting of tori, and $S \subset M$ a properly embedded surface. We use the notation $M\backslash\backslash S$ to denote the path–metric closure of $M \setminus S$. Up to homeomorphism, $M\backslash\backslash S$ is the same as the complement of a regular neighborhood of S.

The *parabolic locus* P is the portion of ∂M that remains in $\partial(M\backslash\backslash S)$. If every torus of ∂M is cut along S, then the parabolic locus P will consist of annuli. Otherwise, it will consist of annuli and tori. The remaining, non-parabolic boundary $\partial(M\backslash\backslash S) \setminus \partial M$ can be identified with $\widetilde{S}$, the boundary of a regular neighborhood of S. In the special case where $M = S^3 \setminus K$ is a link complement and $S = S_\sigma$ is a state surface, we use the notation M_σ to refer to $M\backslash\backslash S_\sigma = (S^3 \setminus K)\backslash\backslash S_\sigma = S^3\backslash\backslash S_\sigma$.

The following lemma recounts a standard argument. It should be compared, for example, to [5, Lemma 2.1].

Lemma 2.2. *Let M be a compact orientable 3–manifold with ∂M consisting of tori. Let $S \subset M$ be a properly embedded essential surface such that ∂S meets every component of ∂M. If S has an accidental parabolic, then there is an embedded essential annulus $A \subset M\backslash\backslash S$ with one boundary component on $\widetilde{S}$ and the other on the parabolic locus $P = \partial M\backslash\backslash\partial S$. Furthermore, the component $\partial A \subset P$ is parallel to a component of $\partial\widetilde{S}$.*

Proof. If S admits an accidental parabolic, then there exists a non-peripheral closed curve γ on S which is freely homotopic into ∂M through M. The free homotopy defines a map of an annulus A_1 into M, with one boundary component on γ and the other on ∂M. Put A_1 into general position with respect to S. Because S may be non-orientable, we will work with the boundary of a regular neighborhood of S, denoted $\widetilde{S}$. We may move the component of ∂A_1 on $\widetilde{S}$ in a bi-collar of S to be disjoint from $\widetilde{S}$. Now, any closed curve of intersection of A_1 and $\widetilde{S}$ that bounds a disk in A_1 can be pushed off $\widetilde{S}$ by the fact that $\widetilde{S}$ is incompressible (because S is essential, Definition 1.1). Likewise, we can push off any arcs of intersection of A_1 and $\widetilde{S}$ which have both endpoints on ∂M, because $\widetilde{S}$ is boundary incompressible. Because we have moved the other boundary component of A_1 off $\widetilde{S}$, there can be no arcs of intersection of A_1 and $\widetilde{S}$. There may be closed curves of intersection that are essential on A_1.

Apply a homotopy to minimize the number of closed curves of intersection. Then there is a sub-annulus $A_2 \subseteq A_1$ that is outermost, i.e. has one boundary component on ∂M, and one on $\widetilde{S}$. Note A_2 might equal A_1. By construction, the interior of A_2 is mapped to the interior of $M \backslash\backslash \widetilde{S}$. We may assume that the mapping of A_2 into $M \backslash\backslash \widetilde{S}$ is non-degenerate, i.e. cannot be homotoped into the boundary of $(M \backslash\backslash \widetilde{S})$, for otherwise the map of A_1 into M can be simplified by homotopy. Now, the annulus theorem of Jaco [16, Theorem VIII.13] implies there exists an essential embedding of an annulus A into $M \backslash\backslash \widetilde{S}$, with one end in $\widetilde{S}$ and the other end on the parabolic locus P.

Now $M \backslash\backslash \widetilde{S}$ is the disjoint union of an I–bundle over S and a manifold homeomorphic to $M \backslash\backslash S$, with the non-parabolic portions of $M \backslash\backslash S$ homeomorphic to the non-parabolic portions of $M \backslash\backslash \widetilde{S}$. The I–bundle over S cannot contain any accidental parabolic annuli, for such an annulus would realize a homotopy between a peripheral and a non-peripheral curve in S. Thus A must lie in the component of $M \backslash\backslash \widetilde{S}$ which is homeomorphic to $M \backslash\backslash S$. □

In [13], we constructed a polyhedral decomposition of M_σ. In the next section, we will outline several of its pertinent features, while referring to [13, 14] for details. To handle the case where K is a knot, we mainly need the following result.

Theorem 2.3 (Theorem 3.23 of [13])**.** *Let $D(K)$ be a connected diagram with an adequate, homogeneous state σ. There is a decomposition of M_σ into 4–valent, checkerboard colored ideal polyhedra. The ideal vertices lie on the parabolic locus P, the white faces are glued to other polyhedra, and the shaded faces lie in $\widetilde{S_\sigma}$, the non-parabolic part of ∂M_σ.*

Normal surface theory ensures that the intersections of the annulus A of Lemma 2.2 with the polyhedral decomposition of M_σ can be taken to have a number of nice properties.

Definition 2.4. We say a surface is in *normal form* if it satisfies the following conditions:

(i) Each component of its intersection with the polyhedra is a disk.
(ii) Each disk intersects a boundary edge of a polyhedron at most once.
(iii) The boundary of such a disk cannot enter and leave an ideal vertex through the same face of the polyhedron.
(iv) The surface intersects any face of the polyhedra in arcs.
(v) No such arc can have endpoints in the same ideal vertex of a polyhedron, nor in a vertex and an adjacent edge.

Lemma 2.5. *Let $D(K)$ be a link diagram with an adequate, homogeneous state σ. Suppose the state surface S_σ has an accidental parabolic. Then the embedded annulus A of Lemma 2.2 can be moved by isotopy into normal form with respect to the polyhedral decomposition of $S^3 \backslash\backslash S_\sigma$. The intersections of A with white faces of the polyhedra are all lines running from one boundary component of A to the other.*

Proof. Note that $M_\sigma = S^3 \backslash\backslash S_\sigma$ is topologically a handlebody, hence irreducible. By Haken [15] we may isotope A into normal form. Consider the intersections of A with white faces. A component of intersection cannot be a simple closed curve, by item (iv) of the definition of normal form. If a component of intersection is an arc with both endpoints on $N(K)$, we can remove this intersection by [13, Lemma 3.20]: every white face of the polyhedral decomposition is boundary incompressible in $M\backslash\backslash S_\sigma$. Similarly, an arc of intersection has both endpoints on S_σ, then we may pass to an outermost such arc and obtain a *normal bigon*, that is a normal disk with two sides. This contradicts [13, Proposition 3.24]: the polyhedral decomposition of $M\backslash\backslash S_\sigma$ contains no normal bigons. □

We are now ready to prove that an adequate, homogeneous state surface for a *knot* admits no accidental parabolics.

Theorem 2.6. *Let $D(K)$ be a knot diagram with an adequate, homogeneous state σ. Then the state surface S_σ cannot be accidental.*

Proof. Suppose not: suppose S_σ is accidental. Then Lemma 2.2 implies there is an embedded annulus A in M_σ with one boundary component on $\widetilde{S_\sigma}$ and the other on the parabolic locus $N(K)$. Consider the intersections of A with a fixed white face W. Because the boundary component of A on $N(K)$ runs parallel to S_σ, the annulus A must intersect each ideal vertex of W. Moreover, by Lemma 2.5, any component of intersection $A \cap W$ runs from the component of A on $N(K)$ to the component on $\widetilde{S_\sigma}$. Hence on W, this intersection is an arc from an ideal vertex of W to one of the sides of W (shaded faces are on $\widetilde{S_\sigma}$).

Because A is normal, item (v) of Definition 2.4 implies that such an arc cannot run from an ideal vertex to an adjacent edge. But now we have a contradiction: there is no way to embed a collection of arcs in W such that each arc meets one ideal vertex and one side of W without having an arc that runs from an ideal vertex to an adjacent edge. □

3. Details of the ideal polyhedra

The proof of Theorem 2.6 for links requires knowing more information about the the polyhedral decomposition of [13]. In this section, we review some of the relevant features, referring to [13, Chapters 2–4] for more details.

A *non-prime arc* is an arc with both endpoints on the same state circle of H_σ, which separates the subgraph of H_σ on one side of the state circle into two graphs which each contain segments. Such a subgraph is called a *non-prime half–disk*. A collection of non-prime arcs is called *maximal* if, once we cut along all such arcs and all state circles, the graph decomposes into subgraphs each of which contains a segment, and no larger collection of non-prime arcs has the same property.

Let $\{\alpha_1, \dots, \alpha_n\}$ denote a maximal collection of non-prime arcs. We define a *polyhedral region* to be a nontrivial region of the complement of the state circles and the α_i. The manifold $M_\sigma = S^3\backslash\backslash S_\sigma$ decomposes into one upper polyhedron and several lower polyhedra. Each lower polyhedron corresponds to precisely one of these polyhedral regions. Furthermore, the state circles and segments that meet this polyhedral region naturally define a subgraph of H_σ and a prime, alternating sub-diagram of $D(K)$. The 1–skeleton of the lower polyhedron is exactly the same as the 4–valent projection graph of the prime, alternating link diagram corresponding to this subgraph of H_σ.

Our maximal collection of non-prime arcs ensures that the polyhedral regions correspond to prime sub-diagrams of $D(K)$ and to lower polyhedra without normal bigons. Meanwhile, the vertices, edges, and faces of the upper polyhedron have the following description.

(1) Each white face corresponds to a (nontrivial, i.e. non-innermost disk) complementary region of $H_\sigma \cup (\cup_{i=1}^n \alpha_i)$.
(2) Each shaded face lies on $\widetilde{S_\sigma}$, and is the neighborhood of a tree that we call a *spine*. The spine is *directed*, in that each edge has a natural orientation. Innermost disks are sources. Arrows are attached corresponding to *tentacles*, which run from a state circle adjacent to a segment (the *head*) and then turn left (all–A case) or right (all–B case) and have their *tail* along a state circle, as well as *non-prime switches*, where four arrows meet at a non-prime arc. See [13, Figure 3.7] for an illustration of these terms.

    When an arc is running through the directed spine in the direction of the arrows, we say it is running *downstream*.
(3) Each vertex of the upper polyhedron corresponds to a strand of $D(K)$ between consecutive under-crossings. In the graph H_σ, this strand follows a *zig-zag*, that is, an alternating sequence of portions of state circles and segments (possibly zero segments). See Figure 4, right, for a zig-zag with one segment.
(4) Each edge of the upper polyhedron starts at the head of a tentacle of a shaded face. As a result, ideal edges can be given an orientation, which matches the orientation of the directed spine in that tentacle.

White faces of the lower polyhedra are glued to white faces of the upper polyhedron. We may transfer combinatorial information about the upper polyhedron into the lower ones via a map called the clockwise map.

Definition 3.1. Let W be a white face of the upper polyhedron, with n sides. If W belongs to an all–A polyhedral region, the *clockwise map* ϕ on W is defined by composing the gluing map of the white face with a $2\pi/n$ clockwise rotation. See Figure 3. If W belongs to an all–B polyhedral region, the map ϕ is defined by composing the gluing map with a $2\pi/n$ counter-clockwise rotation. We sometimes call it the *counter-clockwise map*.

As illustrated in Figure 3, the clockwise or counter-clockwise map ϕ is orientation–preserving. This is because the "viewer" is in the upper polyhedron: we see the boundary of the upper polyhedron from the inside, and each lower polyhedron from the outside. With this convention, the gluing map preserves orientations, hence ϕ does also.

If the special case where $D(K)$ is prime and alternating, there is exactly one lower polyhedron, and the 1–skeleta of both the upper and lower polyhedra coincide with the 4–valent graph of the diagram. In this case, both the clockwise and counter-clockwise maps can be seen as the "identity map" on regions of the diagram [18]. In the non-alternating setting, more details about the clockwise map can be found in [13, Sections 4.2 and 4.5].

The following lemma describes the effect of the clockwise and counterclockwise maps on *normal squares*, that is, normal disks with four sides. Here we allow a portion of the quadrilateral that runs over $N(K)$ (i.e. a neighborhood of an ideal vertex of the polyhedral decomposition) to count as a side.

Lemma 3.2. *Let U be a polyhedral region of the projection plane, let $W_1, \dots, W_k$ be the white faces in U, and let P' be the lower polyhedron associated to U. Then the clockwise (counter-clockwise) map $\phi\colon W_1 \cup \dots \cup W_k \to P'$ has the following properties:*

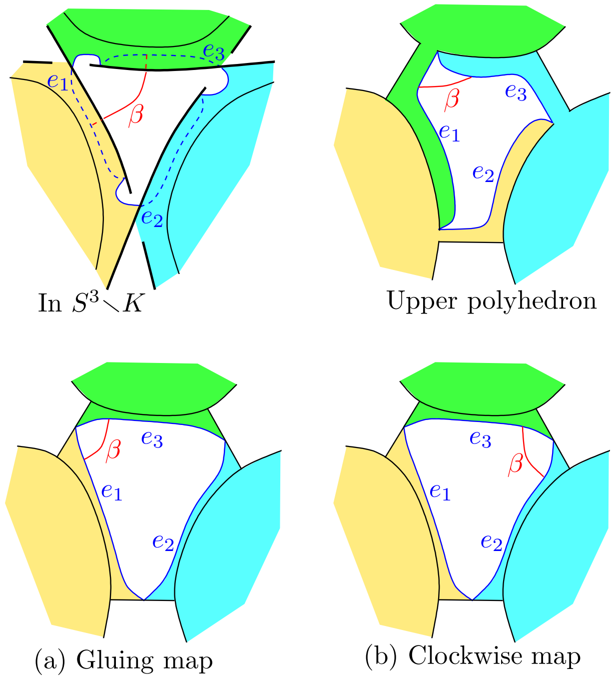

FIGURE 3. An arc β and its image under the gluing map and the clockwise map.

(1) If x and y are points on the boundary of white faces in U that belong to the same shaded face of the upper polyhedron, then $\phi(x)$ and $\phi(y)$ belong to the same shaded face of P'.

(2) Let S be a normal square in the upper polyhedron with two sides on shaded faces (that is, on $\widetilde{S_\sigma}$) and two sides on white faces V and W, with V and W both belonging to polyhedral region U. Let $\beta_v = S \cap V$ and $\beta_w = S \cap W$. Then the arcs $\phi(\beta_v)$ and $\phi(\beta_w)$ can be joined along shaded faces to give a normal square $S' \subset P'$, defined uniquely up to normal isotopy. Write $S' = \phi(S)$.

(3) Let S be a square in the upper polyhedron with one side on a shaded face, two sides on white faces V and W, and the fourth side on $N(K)$, meeting the upper polyhedron in a single ideal vertex between V and W. Suppose further that V and W both belong to polyhedral region U. Then the arcs $\beta_v = S \cap V$ and $\beta_w = S \cap W$ meet at a single ideal vertex in the lower polyhedron, and their other endpoints can be joined along a shaded face to give a normal square $S' \subset P'$, defined uniquely up to normal isotopy. Write $S' = \phi(S)$.

(4) If S_1 and S_2 are disjoint normal squares in the upper polyhedron, all of whose white faces belong to U, then $\phi(S_1)$ is disjoint from $\phi(S_2)$.

Proof. Items (1) and (2) are proved in [13, Lemma 4.8] in the case where U is an all–A polyhedral region. The proof of the all–B case is identical, with "clockwise" replaced by "counter-clockwise." We do need to prove items (3) and (4).

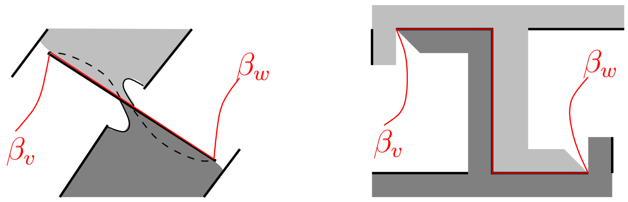

FIGURE 4. Two arcs in white faces in the same all–A polyhedral region, meeting the same ideal vertex, must be as shown. In an all–B region, the picture is mirror reversed.

For (3), let S be a normal square in the upper polyhedron as described: sides β_w and β_v are arcs in white faces V and W lying in U, meeting at a single ideal vertex in the upper polyhedron. The proof of (2) implies that the endpoints of $\phi(\beta_w)$ and $\phi(\beta_v)$ on shaded faces can be connected by an arc in a single shaded face. Thus we focus on the endpoints which lie on an ideal vertex.

Because the clockwise (or counter-clockwise) map takes vertices of white faces to vertices, each of the arcs $\phi(\beta_w)$ and $\phi(\beta_v)$ still has one end on an ideal vertex in P'. We need to verify that they have this end on the same ideal vertex of P'.

Assume, without loss of generality, that U is an all–A polyhedral region, and the map ϕ is clockwise. (The proof for the counter-clockwise map will be identical.)

Recall that an ideal vertex in the upper polyhedron corresponds to a zig-zag in the graph H_σ. Because V and W belong to the same polyhedral region, they are not separated by any state circles. As a result, the vertex between them must be a zig-zag with a single segment. This single segment corresponds to a single over-crossing of the diagram and a single segment of the graph H_σ, as in Figure 4. But now, the clockwise map rotates the vertices of each white face clockwise, to lie in the center of the next segment of H_σ in the clockwise direction. Now, the endpoints of β_v and β_w are rotated to the center of the same segment, namely the segment corresponding to the single over–crossing of the ideal vertex.

Finally, for item (4), as ϕ is a homeomorphism on white faces, sides of $\phi(S_1)$ and $\phi(S_2)$ on white faces are disjoint. If both $\phi(S_1)$ and $\phi(S_2)$ pass through the interior of a shaded face F, then the argument of [13, Lemma 4.8] shows they are disjoint. If $\phi(S_1)$ passes through the interior of a shaded face F and $\phi(S_2)$ passes through a vertex, then they will be disjoint in F. Finally, if $\phi(S_1)$ and $\phi(S_2)$ both pass through ideal vertices of F, if they pass through distinct vertices then their images will be disjoint. If they pass through (a neighborhood of) the same vertex in the upper polyhedron, since the squares are disjoint, in the adjacent white faces the arcs of S_1 must lie on the same side of the arc of S_2. This will be preserved by the clockwise map acting on both faces, and so the images can be connected at the vertex in a manner that keeps them both disjoint. $\square$

4. The case of links

The goal of this section is to prove Theorem 4.1, which generalizes Theorem 2.6 to links with multiple components. We note that, unlike Theorem 2.6, this result needs the hypothesis of prime diagrams.

Theorem 4.1. *Let $D(K)$ be a prime, σ–adequate, σ–homogeneous link diagram. Then the state surface S_σ has no accidental parabolics.*

Suppose, to the contrary, that the state surface S_σ is accidental. Then Lemma 2.2 implies there is an embedded annulus $A \subset M_\sigma$ with one boundary component on $\widetilde{S_\sigma}$ and the other on the parabolic locus $N(K)$. After placing A in normal form (as in Lemma 2.5), we obtain a number of normal squares in individual polyhedra. Following the annulus, these squares $A_1, \ldots, A_n$ alternate lying in the upper polyhedron, then a lower polyhedron, then the upper polyhedron again, and so on. Each A_i has two sides on white faces, one on a shaded face, and one on $N(K)$. Finally, each A_i is glued to A_{i+1} along a white face of the decomposition. Throughout this section, we adopt the convention that odd-numbered squares are in the upper polyhedron.

The proof of Theorem 4.1 is broken up into a number of lemmas, which analyze the intersection pattern of these squares and their clockwise images. In §4.1, we perform the first reductions in the proof and show Proposition 4.4: the annulus A must be composed of at least 4 squares, and some white face met by A has at least 4 sides. Then, in §4.2, we use the conclusion of Proposition 4.4 to restrict the possibilities for $D(K)$ further and further, until we show in §4.3 that S_σ has no accidental parabolics.

4.1. **First reductions in the proof.**

We begin with the following lemma.

Lemma 4.2. *The annulus A must contain at least 4 normal squares.*

Proof. Since the squares A_i alternate between the upper and lower polyhedra, the number of these squares must be even. Thus, suppose A consists of only two squares: A_1 in the upper polyhedron and A_2 in a lower polyhedron. Since A_1 is glued to A_2 along both of its white faces, these white faces V and W must lie in the same polyhedral region U.

By Lemma 3.2 (3), we may map A_1 into the lower polyhedron by a map ϕ. The normal square $A_1' = \phi(A_1)$ runs through one ideal vertex, white faces V and W, and a single shaded face. Without loss of generality, the map ϕ rotates clockwise.

Recall that A_1 is glued to A_2 across V, and that the clockwise map ϕ differs from the gluing map by a $2\pi/n$ rotation. Thus in V, the arc of A_2 differs from that of A_1' by a single clockwise rotation. Similarly in W. Thus the arcs of A_1' and of A_2 in V and W must be as in Figure 5, left. The dashed lines in that figure indicate the clockwise motions of A_2. These must be the lines on the white faces V and W corresponding to A_1'. Note that the points where the dashed lines meet a vertex, labeled x and y, must agree in the polyhedron. Putting these two points together, the diagram must be as in Figure 5, right.

But note in particular that there is a circle coming from the edges of the polyhedra which separates the two endpoints of the solid line representing A_2. (It also separates the two endpoints of the dashed line representing A_1'.) Since these endpoints must be connected by an embedded arc of A_2 in a shaded face, we have a contradiction. □

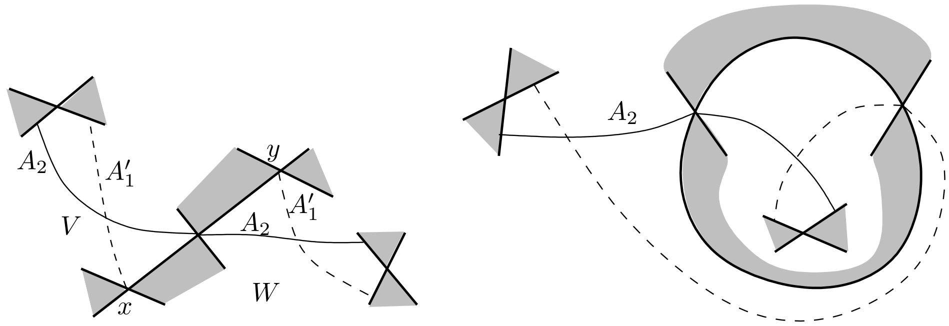

FIGURE 5. A picture of a lower polyhedron, in the case where A is cut into only two squares A_1 and A_2.

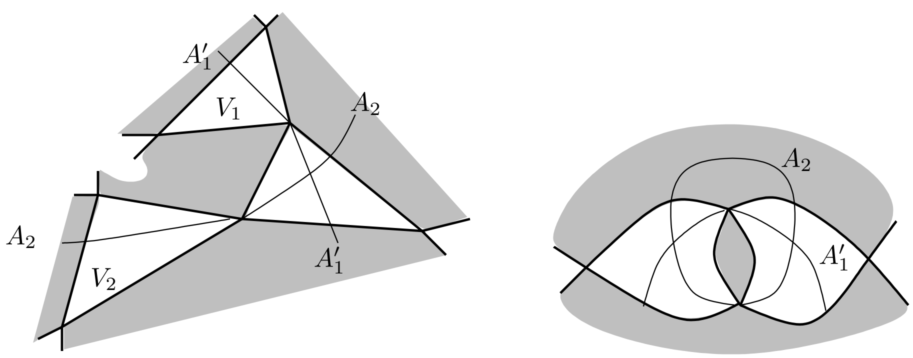

FIGURE 6. Configurations for triangular faces in the same polyhedral region.

Lemma 4.3. *Let $A_1 \subset A$ be a normal square in the upper polyhedron. If both white faces met by A_1 are triangles, these triangles are in different polyhedral regions.*

Proof. Suppose that A_1 lies in the upper polyhedron with both of its white faces in the same polyhedral region, and both of those white faces are triangles. Then we may map A_1 to the lower polyhedron of this polyhedral region via the clockwise (or counter-clockwise) map. Without loss of generality, we may assume that the map ϕ is clockwise in this region. Since A_1 is glued to A_2 and A_n, this lower polyhedron contains both A_2 and A_n.

The square A_2 in a lower polyhedron runs through one shaded face, two triangular white faces, and one ideal vertex. By Lemma 3.2, part (3), $A'_1 = \phi(A_1)$ is also a normal square that passes through an ideal vertex. Because A_1 is glued to A_2, we have one side of A'_1 and one side of A_2 in the same white triangle, and these sides differ by a single clockwise rotation. Thus A'_1 and A_2 must be as shown in Figure 6, left. Note that the shaded face met by A_2 and the shaded face met by A'_1 cannot agree: if they did, this single shaded face would meet the white face along two edges, contradicting [13, Proposition 3.24] (No normal bigons). Hence the arcs shown in that figure can connect to closed curves only if the triangular faces labeled V_1 and V_2 actually coincide.

Since $V_1 = V_2$, the configuration must be as in Figure 6, right. But now, recall that A_1 is glued to square A_n along this white face $V_1 = V_2$. By Lemma 4.2, the squares A_2 and A_n are distinct. Furthermore, since A is embedded, A_2 and A_n are disjoint. However, the side of A_n on the face $V_1 = V_2$ differs from A_1' by a single clockwise rotation. It is impossible for this arc to be disjoint from A_2, which is a contradiction. □

We can now prove the main result of this section.

Proposition 4.4. *The annulus A consists of at least 4 squares. In addition, some white face met by A has at least 4 sides.*

Proof. The first claim in the proposition is proved in Lemma 4.2. To prove the second claim, let $A_1 \subset A$ be a normal square in the upper polyhedron. We will show that this particular normal square meets a white face with at least 4 sides.

First we rule out white faces that are bigons. In a bigon face, each edge is adjacent to each of the two vertices. Thus any arc from an ideal vertex to an edge would violate condition (v) of Definition 2.4, meaning A cannot be normal if it meets a bigon face. This contradiction implies every white face met by A_1 has at least 3 sides.

If both white faces met by A_1 are triangles, then Lemma 4.3 implies these triangles are in different polyhedral regions. To study this situation, we need the following lemma.

Lemma 4.5. *Suppose A_1 is a normal square in the upper polyhedron, with one side on an ideal vertex, two sides on white faces V and W, where V is triangular, and one side, labeled γ, on a shaded face. Label the state circles around V so that ∂A_i runs from a vertex of V on the state circle C_1 to a tentacle whose tail is on the state circle C_2. Then either*

(1) W is inside the region R_1 on the opposite side of C_1 from V; or
(2) W is inside R_2 on the opposite side of C_2 from V.

Furthermore, when we direct γ from V to W, it runs across C_1 or C_2, respectively, running downstream. See Figure 7.

Proof. The square A_1 has one side on the parabolic locus, which is a vertex of the upper polyhedron. Each vertex is a zig-zag. Because A_1 meets a vertex on C_1, part of the zig-zag must lie on C_1.

If all of the zig-zag lies on C_1, that is if the zig-zag consists of a single bit of state surface, then W lies in R_1 on the opposite side of C_1 from V.

If the zig-zag contains one or more segments, then at least one segment of the zig-zag is attached to C_1, on one side or the other. If the segment is attached to C_1 on the side of the region R_1, then W must be inside R_1. (Otherwise, there would be a staircase from state circle C_1 back to C_1, contradicting the Escher Stairs Lemma [13, Lemma 3.4].) If the segment is attached to the side opposite R_1, then because it belongs to a single vertex, it must in fact be the segment labeled s in Figure 7, which connects C_1 to C_2 alongside face V. In this case, the zig-zag includes a portion of C_2, and W will lie on one side or the other of C_2. By the assumption that V and W are in different polyhedral regions, W must lie inside the region R_2 on the opposite side of C_2 from V.

Now we argue that γ runs downstream across C_1 or C_2, when directed away from V towards W. As in Figure 7, the shaded face containing γ is called F_2. For ease of

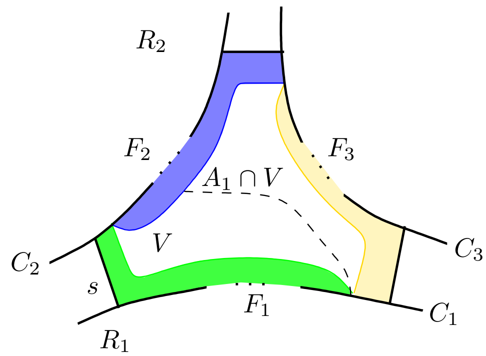

FIGURE 7. Notation for Lemma 4.5. The conclusion of the lemma is that square A_1 must run through shaded face F_2 to a shaded face W contained in region R_1 or region R_2.

exposition, we also refer to F_2 as the blue face. Thus γ starts next to white face V by entering a blue tentacle adjacent to C_2.

First suppose W is in R_2. If γ crosses C_2 immediately from the tail of the blue tentacle, then it must do so running downstream, since only heads of tentacles (rather than no non-prime switches or innermost disks) can attach to tails of tentacles on the opposite side of a state circle. So suppose γ runs upstream into the head of the blue tentacle, crossing state circle C_3. Since C_3 does not separate V and W, in fact γ must cross it twice, and the Utility Lemma [13, Lemma 3.11] implies that γ crosses it first running upstream, then downstream. Between the second time γ crosses C_3 and the first time it crosses C_2, γ must exit out of every non-prime half–disk it enters, else such a disk would separate C_2 and C_3. But no half–disk can separate C_2 and C_3, because they are connected by a segment. Thus the Downstream Lemma [13, Lemma 3.10] implies γ crosses C_2 running downstream.

Finally, suppose W is in R_1. The arc γ begins in a blue tentacle with head on C_3 and tail on C_2. If γ crosses C_2 first, it will be running downstream. But C_2 does not separate V and W in this case, so γ must cross it twice. This contradicts the Utility Lemma. Thus γ crosses C_3 first, running upstream. Again it crosses C_3 twice, and by the Utility Lemma, the second crossing of C_3 occurs running downstream. Then, as in the previous paragraph, the Downstream Lemma implies that γ crosses C_1 running downstream. $\square$

Now we finish the proof of Proposition 4.4.

Let the notation be as in Lemma 4.5. In addition, as Figure 7, let F_i be the shaded face that has a tentacle lying on state circle C_i. Thus γ runs through shaded face F_2.

To finish the proof, we pull a side of A_1 off the parabolic locus, i.e. off the ideal vertex, and into shaded face F_1 or F_3. This creates a normal square with two white sides and two shaded sides.

If W is in R_1, pull A_1 off the ideal vertex and into the tentacle of F_1, to obtain an arc $\sigma \subset F_1$. This arc σ must run downstream across C_1, by the Utility Lemma[13, Lemma 3.11] and Downstream Lemma [13, Lemma 3.10] (as in the above argument).

If W is in R_2, pull A_1 off the ideal vertex and into the tentacle of F_3, obtaining an arc $\sigma \subset F_3$. Again the arc σ must run downstream across C_2.

In either case, we have arcs γ and σ which run downstream from the same state circle (either C_1 if $W \subset R_1$, or C_2 if $W \subset R_2$). They terminate in the same white face, namely W. This contradicts the Parallel Stairs Lemma [13, Lemma 3.14]. $\square$

4.2. **Annuli and squares.** In the next sequence of lemmas, we use Proposition 4.4 to set up the proof that the state surface S_σ has no accidental parabolics. The overall theme of the proof is that each successive lemma places stiffer and stiffer restrictions on the annulus A, the polyhedral decomposition, and the diagram $D(K)$. In the end, we will reach a contradiction.

So far, we have an essential annulus $A \subset M_\sigma$, composed of normal squares $A_1, \ldots, A_n$. Each of these squares has two sides on white faces, one on a shaded face, and the final side on an ideal vertex.

In the arguments below, it is actually easier to view the pieces of A as squares with two sides on shaded faces and two sides on white faces. This is accomplished as follows. Recall that the parabolic locus $\partial N(K) \backslash\backslash S_\sigma$ consists of annuli. One of the boundary circles of A is embedded on one of these parabolic annuli. We may isotope A slightly through M_σ, to move the boundary circle of A from the parabolic locus and onto $\widetilde{S_\sigma}$.

In the polyhedral decomposition, the pushed-off copy of A will be cut into a collection of normal squares with two sides on white faces and two sides on shaded faces, such that one side on a shaded face cuts off a single ideal vertex. We denote these squares by $S_1, \ldots, S_n$. Note each S_i is obtained by pulling A_i off an ideal vertex and into an adjacent shaded face.

In fact, there are two different directions in which we may pull A off the parabolic locus. We make the choice as follows.

Convention 4.6. Let V be a white face with four or more vertices, which meets the annulus A. (The existence of such a white face is guaranteed by Proposition 4.4.) We arrange the labeling of normal squares A_i so that square A_1 in the upper polyhedron is glued along V to square A_2 in some lower polyhedron.

The normal square A_1 meets a vertex of V, which means that one component of $V \setminus A_1$ has two or more vertices. We pull A off the parabolic locus in the direction of this (larger) component of $V \setminus A_1$. Thus, if S_1 is the normal square corresponding to A_1, the arc $S_1 \cap V$ has at least two vertices on each side.

Lemma 4.7. *The annulus A intersects only two white faces, V and W, which belong to the same polyhedral region. Furthermore, every normal square S_i intersects V and W in a way that cuts off at least two vertices on each side.*

Proof. Let V be the white face of Convention 4.6, and let A_1 and S_1 be the corresponding normal squares. Let W be the other white face met by S_1. Since S_1 does not cut off an ideal vertex in V, and is glued to square S_2 across V, [13, Proposition 4.13] implies that V and W are in the same polyhedral region U.[1]

[1] In the monograph [13], Proposition 4.13 and Lemma 4.10 are stated for A–adequate diagrams. As [13, Section 4.5] explains, these results and the other structural results about the polyhedra also apply to σ–adequate, σ–homogeneous diagrams.

Now, Lemma 3.2 part (2) says that we may map S_1 into the lower polyhedron corresponding to U and obtain a normal square $S_1' = \phi(S_1)$. Note that the arc $S_1' \cap V$ will differ from $S_2 \cap V$ by a single rotation, by the definition of the clockwise (or counter-clockwise) map. Since S_1' cuts off more than a single vertex in V, [13, Lemma 4.10] implies that S_1' intersects S_2 nontrivially, in both of its white faces. But this means that S_2 meets both V and W in arcs that cut off more than a single vertex on each side.

The square S_2 is glued along W to a square S_3 in the upper polyhedron. The arc $S_3 \cap W$ cuts off more than a single vertex on each side, because it is glued to S_2. Thus, as above, [13, Proposition 4.13] implies that both white faces of S_3 are in the same polyhedral region U, and [13, Lemma 4.10] implies that $S_3' = \phi(S_3)$ intersects S_2 nontrivially, in both of its white faces. In other words, S_3 meets the same white faces V and W, in arcs that cut off more than a single vertex on each side. Continue in this fashion to obtain the same conclusion for every S_i. □

Let S_i be an even-numbered square in a lower polyhedron. Lemma 4.7 tells us that S_i is glued to S_{i-1} across V and to S_{i+1} across W, where V and W are the same as i varies.

Definition 4.8. To continue studying the intersection patterns of normal squares in the lower polyhedron, we define

$$T_i = \begin{cases} \phi(S_i) & \text{if } i \text{ is odd} \\ S_i & \text{if } i \text{ is even.} \end{cases}$$

Note that every T_i lives in the lower polyhedron of the polyhedral region U.

For every square T_i, we label its four sides as follows. The sides of T_i in white faces V and W are denoted v_i and w_i, respectively. One shaded side of S_i was created by pulling a side of A_i off the parabolic locus; the corresponding side of T_i is denoted p_i. (Note that by Lemma 3.2, part (3), if an odd-numbered square S_i in the upper polyhedron has a shaded side that cuts off an ideal vertex, then so does $T_i = \phi(S_i)$.) We will orient the arcs v_i and w_i so that they point toward p_i, and orient p_i from v_i toward w_i. That is, p_i is oriented from V to W.

Similarly, an odd-numbered square S_i in the upper polyhedron also contains an arc q_i that was pulled off the parabolic locus. As before, we orient q_i from V to W.

Lemma 4.9. *Let i be even, so that $S_i = T_i$ is in a lower polyhedron, and suppose that we pulled S_i off an ideal vertex that lies to the right of p_i. Then*

(1) $v_{i-1} = \phi(v_i)$ and $w_{i+1} = \phi(w_i)$, with orientations preserved.
(2) $p_{i\pm1}$ cuts off an ideal vertex to its right.
(3) In the upper polyhedron, $q_{i\pm1}$ also cuts off an ideal vertex to its right.

Proof. By construction, $v_i \subset S_i$ is glued to an arc of $S_{i-1} \cap V$, whose image under ϕ is v_{i-1}. Similarly for w_i and w_{i+1}. Since ϕ is orientation–preserving, (1) follows.

Conclusion (2) follows immediately from Lemma 3.2 part (3) because S_i was created by pulling A_i off an ideal vertex in a direction that is consistent for all i. Similarly, conclusion (3) follows from Lemma 3.2 part (3) because ϕ is orientation–preserving. □

Lemma 4.10. *Each square T_i encircles a bigon shaded face of the lower polyhedron.*

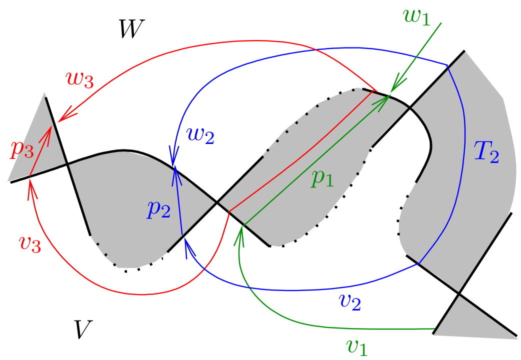

FIGURE 8. Proof of Lemma 4.10: squares T_1, T_2, and T_3 must meet a lower polyhedron as shown.

Proof. Assume without loss of generality that V and W are in an all–A polyhedral region. We may also assume without loss of generality that p_2 was created by pulling A_2 off an ideal vertex so that the vertex lies to the right of p_2. (Otherwise, interchange the labels of faces V and W, reversing the order of the indices and the orientation on every p_i.)

By Lemma 4.9, the arc v_1 is clockwise from v_2 in face V, and w_3 is clockwise from w_2 in face W. Moreover, v_2 intersects both v_1 and v_3, and similarly w_2 intersects both w_1 and w_3. But $T_1 = \phi(S_1)$ and $T_3 = \phi(S_3)$ are clockwise images of disjoint squares, hence are disjoint by Lemma 3.2 (4). Thus T_1, T_2, and T_3 must be as shown in Figure 8. In particular, p_1 and T_3 run parallel through the same shaded face. Dotted lines in the figure indicate that the boundary of the corresponding shaded face may meet additional vertices.

The arc p_2 cuts off an ideal vertex to its right, so by Lemma 4.9, the arcs p_1 and p_3 also cut off ideal vertices to their right. Thus the dotted line to the right of p_1 in Figure 8 must actually be solid. By primeness of the lower polyhedron, all other dotted lines must also be solid. Thus both T_2 and T_3 each encircle a single bigon shaded face.

We may repeat the above argument with T_{2k} taking the place of T_2, for any k, hence each T_i encircles a bigon. □

Lemma 4.11. *The white faces V and W met by annulus A are the only white faces of the polyhedral decomposition. As a consequence, $D(K)$ is the standard diagram of a $(2, n)$ torus link, and S_σ is an annulus.*

Proof. Recall that by Lemma 4.7, there is a polyhedral region U containing white faces V and W, such that every normal square S_i passes through V and W. These normal squares define squares T_i in the lower polyhedron, as in Definition 4.8. By Lemma 4.10, every T_i encircles a bigon shaded face of this lower polyhedron. The number of these bigons is n, the same as the number of normal squares in A.

This is enough to conclude that all the shaded faces of the lower polyhedron corresponding to U are bigons, chained end to end. Thus V and W are the only white faces of this lower polyhedron. The 1–skeleton of this lower polyhedron coincides with the standard diagram of a $(2, n)$ torus link, as on the left of Figure 9.

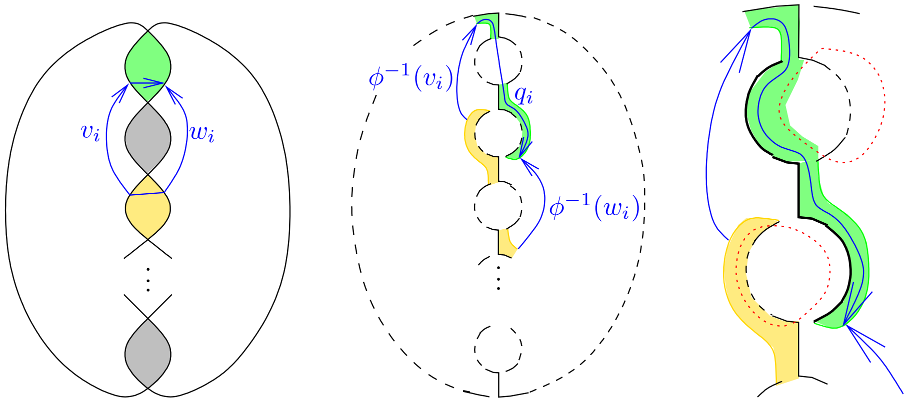

FIGURE 9. Proof of Lemma 4.11. Left: T_i encircles a bigon in the lower polyhedron. Center: The clockwise preimage $S_i = \phi^{-1}(T_i)$ in the upper polyhedron. Right: The ideal vertex cut off by S_i.

If the diagram $D(K)$ is prime and alternating, there is only one lower polyhedron, whose 1–skeleton corresponds to $D(K)$. Thus $D(K)$ is the standard diagram of a $(2, n)$ torus link, where n is even. The rest of the argument reduces us to this case.

In the general case, the upper polyhedron may be more complicated. However, one polyhedral region in the upper polyhedron looks like that of a $(2, n)$ torus link, as in the middle panel of Figure 9. A priori, there may be additional segments attached to the opposite sides of all state circles involved. This is indicated in that figure by the dashed lines along state circles.

For each square T_i in the lower polyhedron, label three sides of T_i by v_i, w_i, and p_i, as in Lemma 4.9. Focusing attention on $T_2 = S_2$, we may assume that arc p_2 in a shaded face was pulled off an ideal vertex to its right. (Otherwise, as in Lemma 4.10, switch the labels of V and W.) Applying Lemma 4.9 part (2) inductively, we conclude that for each even index j, arc p_j was pulled off an ideal vertex to its right.

Now, let i be an odd index, so that S_i is a square in the upper polyhedron. Since T_i encircles an ideal bigon, as in Figure 9, the clockwise preimage $S_i = \phi^{-1}(T_i)$ must be as in the middle panel of Figure 9. By Lemma 4.9, the arc q_i of S_i that was pulled off the parabolic locus must cut off an ideal vertex to its right. This means that portions of state circles adjacent to q_i to its right must actually be solid, to form a single zig-zag, with no segments to break it up. In other words, we have the third panel of Figure 9. The third panel of Figure 9 shows two dotted closed curves, each meeting the link diagram exactly twice. Using the hypothesis that the diagram is prime, each of these closed curves cannot enclose segments (which would correspond to crossings of the diagram).

We conclude that two consecutive state circles in H_σ are innermost, and contain no additional polyhedral regions. Repeating the same argument for the next odd-numbered square S_{i+2} leads to the conclusion that the next two state circles in H_σ are also innermost. Continuing in this way, we conclude that there is only one polyhedral region, which corresponds to the diagram of a $(2, n)$ torus link. $\square$

4.3. **Completing the proofs.** We are now ready to prove Theorem 4.1 and Theorem 1.6.

Proof of Theorem 4.1. Suppose that S_σ has an accidental parabolic. Then Lemma 2.2 implies there is an embedded essential annulus $A \subset S^3 \backslash\backslash S_\sigma$. By Lemma 4.7, A intersects only two white faces, V and W. By Lemma 4.11, V and W are the only faces of the polyhedral decomposition, hence $D(K)$ is the standard diagram of a $(2, n)$ torus link and S_σ is an annulus.

Note that the only non-trivial simple closed curve in an annulus is boundary–parallel. Therefore, the component of ∂A that lies on $\widetilde{S_\sigma}$ is actually parallel to $\partial \widetilde{S_\sigma}$. This contradicts the assumption that A is an essential annulus realizing an accidental parabolic. □

Proof of Theorem 1.6. By [13, Theorem 3.25], S_σ is essential in $S^3 \setminus K$, and by Theorem 4.1 it has no accidental parabolics. By [13, Theorem 5.21] (or [12]) S_σ is a fiber in $S^3 \setminus K$ if and only if G'_σ is a tree. Furthermore, by [13, Theorem 5.21], if S_σ lifts to a fiber in a double cover of $S^3 \setminus K$, then M_σ is an I–bundle, hence G'_σ is a tree.

It follows that if K is hyperbolic, the surface S_σ is quasifuchsian if and only if the reduced state graph G'_σ is not a tree. □

References

[1] Colin C. Adams, *Noncompact Fuchsian and quasi-Fuchsian surfaces in hyperbolic 3–manifolds*, Alebr. Geom. Topol. **7** (2007), 565–582.

[2] Francis Bonahon, *Bouts des variétés hyperboliques de dimension* 3, Ann. of Math. (2) **124** (1986), no. 1, 71–158.

[3] Richard D. Canary, David B. A. Epstein, and Paul Green, *Notes on notes of Thurston*, Analytical and geometric aspects of hyperbolic space (Coventry/Durham, 1984), London Math. Soc. Lecture Note Ser., vol. 111, Cambridge Univ. Press, Cambridge, 1987, pp. 3–92.

[4] Jae Choon Cha and Charles Livingston, *Knotinfo: Table of knot invariants*, `http://www.indiana.edu/~knotinfo`, 2011.

[5] Daryl Cooper and Darren D. Long, *Some surface subgroups survive surgery*, Geom. Topol. **5** (2001), 347–367 (electronic).

[6] Peter R. Cromwell, *Homogeneous links*, J. London Math. Soc. (2) **39** (1989), no. 3, 535–552.

[7] Oliver T. Dasbach, David Futer, Efstratia Kalfagianni, Xiao-Song Lin, and Neal W. Stoltzfus, *The Jones polynomial and graphs on surfaces*, Journal of Combinatorial Theory Ser. B **98** (2008), no. 2, 384–399.

[8] Oliver T. Dasbach and Xiao-Song Lin, *On the head and the tail of the colored Jones polynomial*, Compositio Math. **142** (2006), no. 5, 1332–1342.

[9] Sérgio R. Fenley, *Quasi-Fuchsian Seifert surfaces*, Math. Z. **228** (1998), no. 2, 221–227.

[10] Elizabeth Finkelstein and Yoav Moriah, *Tubed incompressible surfaces in knot and link complements*, Topology Appl. **96** (1999), no. 2, 153–170.

[11] ———, *Closed incompressible surfaces in knot complements*, Trans. Amer. Math. Soc. **352** (2000), no. 2, 655–677.

[12] David Futer, *Fiber detection for state surfaces*, Alg. Geom. Topol. (to appear), arXiv:1201.1643.

[13] David Futer, Efstratia Kalfagianni, and Jessica Purcell, *Jones polynomials, volume, and essential knot surfaces: a survey*, Proceedings of Knots in Poland III, Banach Center Publications (to appear), arXiv:1110.6388.

[14] David Futer, Efstratia Kalfagianni, and Jessica S. Purcell, *Guts of surfaces and the colored Jones polynomial*, Lecture Notes in Mathematics, vol. 2069, Springer, 2013, arXiv:1108.3370.

[15] Wolfgang Haken, *Theorie der Normalflächen*, Acta Math. **105** (1961), 245–375.

[16] William Jaco, *Lectures on three-manifold topology*, CBMS Regional Conference Series in Mathematics, vol. 43, American Mathematical Society, Providence, R.I., 1980.
[17] Louis H. Kauffman, *State models and the Jones polynomial*, Topology **26** (1987), no. 3, 395–407.
[18] Marc Lackenby, *The volume of hyperbolic alternating link complements*, Proc. London Math. Soc. (3) **88** (2004), no. 1, 204–224, With an appendix by Ian Agol and Dylan Thurston.
[19] W. B. Raymond Lickorish and Morwen B. Thistlethwaite, *Some links with nontrivial polynomials and their crossing-numbers*, Comment. Math. Helv. **63** (1988), no. 4, 527–539.
[20] Joseph D. Masters and Xingru Zhang, *Closed quasi-Fuchsian surfaces in hyperbolic knot complements*, Geom. Topol. **12** (2008), no. 4, 2095–2171.
[21] William Menasco and Alan W. Reid, *Totally geodesic surfaces in hyperbolic link complements*, Topology '90 (Columbus, OH, 1990), Ohio State Univ. Math. Res. Inst. Publ., vol. 1, de Gruyter, Berlin, 1992, pp. 215–226.
[22] Makoto Ozawa, *Essential state surfaces for knots and links*, J. Aust. Math. Soc. **91** (2011), no. 3, 391–404.
[23] Józef H. Przytycki, *From Goeritz matrices to quasi-alternating links*, The mathematics of knots, Contrib. Math. Comput. Sci., vol. 1, Springer, Heidelberg, 2011, pp. 257–316.
[24] Morwen Thistlethwaite and Anastasiia Tsvietkova, *An alternateive approach to hyperbolic structures on link complements*, arXiv:1108.0510.
[25] Morwen B. Thistlethwaite, *On the Kauffman polynomial of an adequate link*, Invent. Math. **93** (1988), no. 2, 285–296.
[26] William P. Thurston, *The geometry and topology of three-manifolds*, Princeton Univ. Math. Dept. Notes, 1979.
[27] Yukihiro Tsutsumi, *Hyperbolic knots spanning accidental Seifert surfaces of arbitrarily high genus*, Math. Z. **246** (2004), no. 1-2, 167–175.
[28] Anastasiia Tsvietkova, *Hyperbolic structures from link diagrams*, Ph.D. thesis, University of Tennessee, 2012.
[29] Daniel T. Wise, *Subgroup separability of the figure 8 knot group*, Topology **45** (2006), no. 3, 421–463.
[30] Ying-Qing Wu, *Incompressible surfaces in link complements*, Proc. Amer. Math. Soc. **129** (2001), no. 11, 3417–3423 (electronic).

Department of Mathematics, Temple University, Philadelphia, PA 19122, USA
E-mail address: `dfuter@temple.edu`

Department of Mathematics, Michigan State University, East Lansing, MI 48824, USA
E-mail address: `kalfagia@math.msu.edu`

Department of Mathematics, Brigham Young University, Provo, UT 84602, USA
E-mail address: `jpurcell@math.byu.edu`